



Corrosion and Safety of a Ship: Survey Report of a Long-Life Ship

M. Arita, H. Inoue, E. Fuji and T. Kobayashi, Ship Research Institute, Tokyo, Japan

ABSTRACT

A 56 years old ship, *K-maru*, was investigated for items being concerned with her strength. Items investigated were the thickness of shell and deck plates, local and overall deformation of the hull, the wear of rivet heads and mechanical and other properties of steel plates of decks and hull. The characteristics of old plates investigated were chemical compositions, static and dynamic tensile strength, fracture toughness and fatigue strength. Thickness distribution of old plates with worn out holes due to corrosion were also measured.

Based on the results of investigations, the seaworthiness of *K-maru* was discussed. Results obtained were as follows;

1. The plate thickness reduction rate by corrosion of decks and shell plates at midship was about 5% in spite of her old age, though there existed some deep corroded parts in them.
2. The 5% of the whole hull deterioration rate corresponded to about 0.6% corrosion hole area ratio of the whole hull.
3. A small amount of deformation of the ship hull as a whole was responsible for the long term service and repeated repairs by welding.
4. The original old steel plates of 56 years showed good tensile strength, but poor weldability and fracture toughness.
5. Very rough surfaces of steel plates due to corrosion largely diminished their fatigue lives, because of decrease in thickness and stress concentration by surface roughness.
6. The seaworthiness level of the ship was very low. This level may reveal itself at the time of emergency.

BACKGROUND

The safe navigation characteristics of a steel structure sailing ship *K-maru*, 56-year-old at the time, was investigated. The principal dimensions of the ship were as following.

$L_{OA} \times B \times D \times d = 97.00 \text{ m} \times 12.95 \text{ m} \times 7.85 \text{ m} \times 6.15 \text{ m}$
Gross tonnage = 2244.64 ton.

K-maru was constructed by using rivets, and so the original steel plates used were those without considerations of their weldability.

Figure 1 shows the short history of the navigation of *K-maru*. Annual navigation mileage is 20000 - 25000 nautical miles. And in this mileage, 10000 miles are performed by sailing (shown by solid circles in the figure). In Fig. 2, shaded plates show the side and bottom plates replaced by new ones in the way of her history. Numbers of replaced plates are 40 for port side and 55 for starboard side. In Fig. 3, replacements of deck plates are shown. The first replacement took place at the time when *K-maru* was 47-year-old. Whole plates of long poop deck and 80% of upper-deck were replaced, and no plates of No. 2 and No. 3 decks were replaced at the time of our investigation.

These replacements of decks, side and bottom plates were performed because of excessive local deterioration of plates due to

corrosion. We investigated into the strength of *K-maru* and discussed the safety navigation characteristics of her, because of the anticipation that deterioration might proceed in steel plates which were not yet precisely inspected, and that there might be troubles of welding due to connecting original steel plates and new ones (replacements of side and bottom plates were conducted by using rivets but those of decks and other members other than side and bottom plates were conducted by welding), and also because of the fact that many heads of rivets were severely worn out.

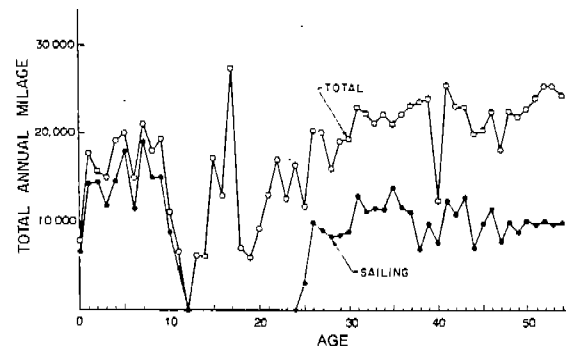


Fig. 1 Navigation History of *K-maru*

METHOD OF INVESTIGATION

Investigations were conducted at two times of docking of *K-maru*. Items of investigations were: amounts of reduction in thickness of plates at midship due to corrosion, overall and local deformations of decks and hull and reduction in volume of rivets due to corrosion. Analysis of chemical compositions, precise measurement of thickness distribution and tests concerning strength were conducted for *K-maru*'s old plates which were replaced by new weldable steel plates.

AMOUNT OF PLATE THICKNESS REDUCTION

Amounts of plate thickness reduction due to corrosion were measured at two points on every plate consisting hull structure at midship by using electromagnetic thickness meter. Table 1 shows the results. In the table, A6, B6 and so on are the names of plates shown in Fig. 2. The plate I8 starboard side was under construction of replacement at the time of investigation. Though there are plates like C8 port and H8 starboard which are corroded excessively, other plates are not so much. Mean values of thickness reduction of most plates are rather small, and the nominal total mean thickness reduction of plates at midship is nearly 5%, though there are plate like G8 and H8 port which have deep locally corroded parts.

Table 1. Plate Thickness at Midship Section

Plate No.		Port Side			Starboard Side		
Name	t_0 (mm)	Age	t	t/t_0	Age	t	t/t_0
Bottom	A6 14.2	55	14.0 13.7	99 % 96 %	55	13.9 13.9	98 % 98 %
	B6 13.2	55	12.7 12.7	96 % 96 %	55	12.7 12.3	96 % 93 %
	C8 13.2	55	11.0 13.1	83 % 83 %	55	12.5 12.6	95 % 95 %
	D6 13.2	11~15	13.2 13.2	100 % 100 %	55	12.5 12.3	95 % 93 %
Bilge	E7 13.2	55	12.9 13.2	98 % 100 %	55	12.9 13.2	98 % 100 %
	F4 13.2	16~20	13.2 13.5	100 % 100 %	1~5	13.7 13.2	100 % 100 %
Ship Side	G8 14.2	55	12.9 12.7	(7.7 * 54%) 89 %	55	13.3 13.2	94 % 93 %
	H8 14.2	55	10.5 13.2	74 % 93 %	55	10.7 13.7	75 % 76 %
	I8 13.2	26~30	12.9 12.7	98 % 96 %	-	-	% %
	J7 13.2	55	13.1 13.0	99 % 98 %	55	13.2 13.2	100 % 100 %
	K7 14.2	26~30	14.2 12.7	100 % 89 %	26~30	14.1 14.2	99 % 100 %
	L8 13.7	26~30	13.7 13.7	100 % 100 %	55	11.4 11.7	83 % 85 %
Mean Value				94.9%			94.8%

t_0 : Original Thickness, t: Thickness, *) local corrosion part

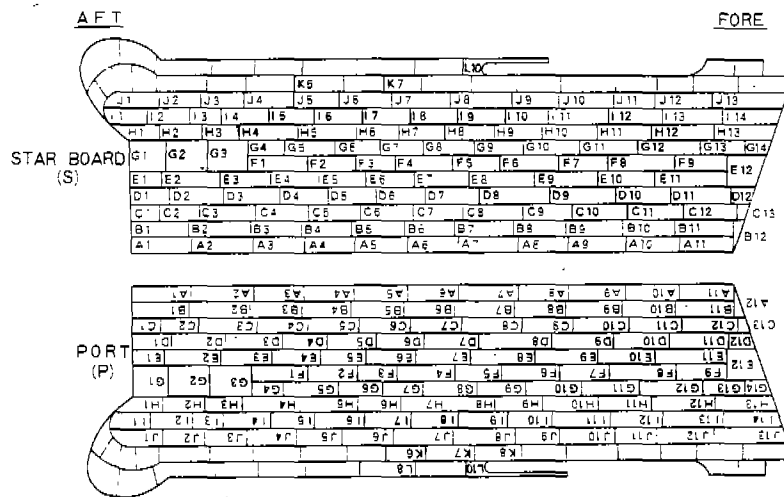


Fig. 2 Replacement of Side Shell Plate (Shaded Plates were replaced at 25 through 56 years old of ship age)

It seemed to be rather controversial that the fact mentioned above and the fact that there found many corrosion holes in deck plates. But this was because that corrosion holes or deep corroded parts were very much isolated and other parts were not so much affected by these.

In order to clarify the characteristics of corrosion hole, we measured the detailed thickness distribution of two old plates (a shell plate and an inner plate attached to a shell plate), both of which had corrosion holes. Tables 2 and 3 show the results of measurement. Plate thicknesses were measured by a large size micrometer at cross points of vertical and horizontal lines which were apart from each other by 20 mm. In the tables shaded parts have plate thickness less than 2 mm, and these parts are possible to be considered as parts of holes. Plate thickness of 2 mm corresponded to 17 - 20% of original one, and surfaces of such plates

showed very rough appearance. And it was difficult to completely eliminate rust from their surfaces. The value 2 mm mentioned above had no theoretical meaning but just for practical purpose.

It is clear from these tables that the area of corrosion holes and directly surrounding excessively thin places are very much limited. Decrease in thickness of parts of the plate somewhat apart from holes, is relatively small. There seems to exist an analogy between the phenomenon mentioned above and the fact that there are many corrosion holes (expressed by corrosion hole ratio V) in spite of rather small amount of mean nominal deterioration due to corrosion (expressed by whole area corrosion ratio Δ) of 5% in Table 1. So we attempted to combine the two phenomenon in order to obtain the relation between V and Δ , by using results in Tables 2 and 3.

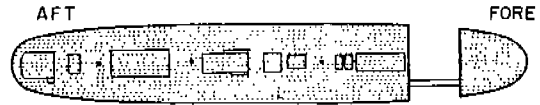
Table 2. Thickness Distribution of a Plate with Corrosion Holes
(Side Shell Plate K-13-P)
Original Thickness = 10.16 mm

	1	2	3	4	5	6	7	8	9	10	11	12	13	14	15	16	17	18	19	20	21	22	23	24	25	26	27	28	29	
A	9.55	9.57	9.62	9.57	9.55	9.56	9.65	9.53	9.55	9.56	9.48	9.46	9.48	9.45	9.47	9.42	9.45	9.48	9.48	9.47	9.48	9.48	9.43	9.50	9.56	9.63	9.63	9.64	9.64	9.62
B	9.38	9.62	9.66	9.63	9.65	9.63	9.70	9.64	9.62	9.64	9.60	9.61	9.57	9.57	9.60	9.73	9.68	9.61	9.59	9.54	9.59	9.54	9.67	9.60	9.56	9.64	9.64	9.65	9.64	9.60
C	9.56	9.63	9.68	9.69	9.62	9.64	9.63	9.65	9.67	9.65	9.64	9.58	9.63	9.60	9.66	9.55	9.57	9.57	9.59	9.54	9.56	9.58	9.67	9.52	9.21	9.10	9.64	7.99	9.81	
D	9.55	9.74	9.87	9.84	9.61	9.64	9.61	9.58	9.57	9.61	9.59	9.56	9.64	9.57	9.53	9.55	9.54	9.64	9.61	9.60	9.52	9.64	9.63	9.28	9.70	9.15	9.47	9.83	9.80	
E	9.47	9.72	9.74	9.65	9.64	9.61	9.58	9.57	9.61	9.59	9.56	9.62	9.56	9.51	9.57	9.54	9.60	9.59	9.62	9.52	9.67	9.67	9.75	9.74	9.09	9.10	7.95	7.81	7.94	
F	9.44	9.70	9.73	9.70	9.62	9.86	9.79	9.91	9.85	9.79	9.99	9.86	9.62	9.56	9.80	9.63	9.53	9.78	9.55	9.25	18.25	10.00	9.12	9.61	9.02	7.28	7.50	9.05	9.26	
G	9.42	9.64	9.65	9.69	9.68	10.00	9.95	9.93	9.81	9.89	9.54	9.78	9.23	9.47	9.84	9.68	9.40	9.10	9.04	9.29	9.68	9.44	9.19	9.95	9.90	7.35	7.81	7.94	9.55	
H	9.50	9.57	9.60	9.63	9.52	9.68	9.78	9.95	9.85	9.75	9.27	9.12	9.02	9.99	9.75	9.60	9.03	9.50	9.60	9.01	9.00	9.00	9.39	9.65	9.49	7.11	8.20	9.27	9.35	
I	9.13	9.76	9.42	9.10	9.30	9.23	9.09	9.72	9.91	9.72	9.11	9.08	9.93	9.50	9.58	7.70	9.46	7.88	7.58	9.48	7.65	7.48	9.51	6.31	6.21	7.72	9.90	9.08	9.71	
J	9.47	9.88	9.17	9.55	9.16	9.27	9.58	9.29	9.76	9.20	9.89	9.14	7.63	6.54	6.22	5.57	5.20	5.06	3.26	4.46	3.39	3.18	4.05	4.30	5.02	9.17	9.26	9.22	9.72	
K	8.79	8.99	9.46	9.01	8.79	8.66	8.50	8.51	8.82	8.59	8.93	9.72	4.02	3.40	2.62	2.91	2.49	2.78	2.49	2.29	2.30	2.54	3.71	4.62	5.75	6.07	8.93	9.11	9.00	
L	7.90	7.55	7.47	7.29	7.30	5.99	6.13	5.00	6.34	4.95	2.97	1.92	1.79	1.25	0.00	1.19	0.70	0.96	1.47	2.25	1.78	1.68	1.47	2.57	5.24	7.77	8.88	9.95	9.92	
M	5.45	3.70	4.26	4.41	4.25	2.45	0.00	3.59	3.94	1.22	0.00	0.00	0.00	0.00	0.00	0.00	0.00	1.39	2.66	2.52	2.52	2.61	2.33	2.64	4.80	7.86	8.64	9.00	9.93	
N	9.18	3.94	3.87	3.63	1.78	2.81	3.34	3.39	3.15	2.62	1.98	1.58	0.00	0.00	0.83	1.15	2.34	6.04	3.70	4.80	6.24	7.11	5.57	5.38	6.40	8.95	9.04	9.22		
O	4.15	2.20	1.60	3.11	2.42	0.09	3.28	3.48	3.94	2.80	1.71	1.25	0.00	2.30	2.64	1.81	1.17	4.48	9.50	8.86	9.70	9.72	9.48	9.70	9.78	9.99	9.02	9.07	9.14	
P	3.44	1.93	2.61	3.91	3.40	3.88	3.20	3.53	3.34	2.90	3.23	3.56	3.81	5.65	6.34	5.85	6.47	9.13	9.69	9.43	9.63	9.47	9.43	9.54	9.48	9.01	9.13	9.07	9.18	
Q	4.83	4.47	4.87	5.00	4.96	3.94	3.95	5.43	5.92	4.35	9.36	7.22	7.20	6.55	6.70	7.83	8.61	9.09	9.66	9.49	9.44	9.62	9.48	9.51	9.48	9.46	9.05	9.22	9.26	9.45
R	8.14	7.60	7.20	6.72	5.78	5.81	6.46	6.04	9.44	9.24	9.04	9.18	9.75	9.43	9.09	9.35	9.55	9.59	9.64	9.56	9.35	9.5								
S	9.08	9.00	7.73	7.88	8.17	8.28	8.88	9.28	9.68	9.72	9.69	9.79	9.61	9.61	9.62	9.52	9.62	9.57	9.51	9.46	9.47	9.5								
T	9.07	9.43	9.34	9.14	8.84	9.27	8.99	9.60	9.56	9.54	9.61	9.23	9.54	9.49	9.58	9.54	9.59	9.58	9.58	9.53	9.53	9.5								
U	9.58	9.63	9.65	9.66	9.38	9.27	9.57	9.55	9.47	9.74	9.10	9.74	9.01	9.47	9.46	9.55	9.57	9.53	9.53	9.54	9.55	9.5								
V	9.41	9.56	9.56	9.27	9.78	9.57	9.58	9.53	9.56	9.49	9.31	9.04	9.47	9.42	9.50	9.51	9.47	9.40	9.58	9.55	9.48	9.6								
W	9.42	9.53	9.54	9.28	9.30	9.47	9.45	9.40	9.52	9.44	9.51	9.51	9.53	9.51	9.53	9.51	9.36	9.45	9.54	9.50	9.45	9.4								
X	9.50	9.65	9.42	9.34	9.31	9.28	9.45	9.59	9.55	9.49	9.44	9.46	9.53	9.51	9.45	9.42	9.16	9.36	9.17	9.39	9.51	9.6								

Table 3. Thickness Distribution of a Plate with Corrosion Holes
(Inner Plate of Side Shell Plate J-13-P)
Original Thickness = 11.68 mm

	1	2	3	4	5	6	7	8	9	10	11	12	13	14	15	16	17	18
A	10.04	10.32	10.15	9.47	9.07	9.59	7.95	7.19	6.65	5.53	4.84	6.23	6.89	7.07	6.88	6.44	6.70	6.70
B	10.30	9.94	9.54	8.42	8.35	8.48	7.52	7.30	4.5	7.05	6.22	5.52	6.95	6.96	7.39	9.53	9.31	10.31
C	10.54	10.91	10.55	10.13	9.63	9.37	8.97	8.84	6.37	6.84	6.14	6.02	6.27	5.87	6.70	10.48	10.52	10.56
D	10.71	10.36	10.50	10.09	9.03	8.40	7.21	5.10	5.17	4.50	3.07	5.63	5.11	6.75	9.50	10.34	10.42	10.61
E	10.41	10.83	10.29	10.15	8.20	5.50	5.56	3.94	3.82	3.34	3.91	4.39	5.02	7.56	10.67	10.48	10.65	10.58
F	10.63	10.91	10.37	10.08	5.09	4.42	5.29	5.29	8.00	1.08	3.38	4.67	4.74	10.09	10.46	10.51	10.55	10.64
G	9.93	10.45	10.31	9.75	5.32	1.81	0.00	1.16	2.43	3.1	5.53	5.56	8.74	10.22	10.47	10.53	10.40	10.43
H	10.00	10.59	10.05	9.98	5.47	0.00	1.44	0.00	1.54	1.69	3.48	5.38	7.78	10.43	10.48	10.45	10.56	10.58
I	10.52	10.43	10.23	10.10	9.63	9.90	0.00	0.00	0.01	1.33	2.72	7.13	9.21	10.29	10.43	10.51	10.55	10.73
J	10.28	10.43	10.95	9.78	9.26	0.00	0.00	0.00	0.00	0.00	0.00	3.23	6.21	9.99	10.19	10.28	10.43	10.55
K	10.11	10.41	9.98	9.71	9.26	0.00	0.00	0.00	0.00	0.00	0.00	2.91	5.71	8.43	10.21	10.27	10.36	10.49
L	10.43	10.46	10.05	9.40	5.27	0.00	0.00	0.00	0.00	0.00	0.00	7.24	9.46	8.42	10.29	10.40	10.26	10.47
M	10.25	10.38	10.19	9.59	5.06	0.00	0.00	0.00	0.00	0.00	0.00	3.35	8.84	8.53	10.37	10.35	10.41	10.42
N	9.96	10.17	10.00	9.83	9.45	0.00	0.00	0.00	0.00	0.00	0.00	3.09	6.78	9.04	10.46	10.46	10.47	10.52
O	10.12	10.41	10.18	9.83	9.70	0.00	0.00	0.00	0.00	0.00	0.00	3.63	7.74	10.40	10.39	10.44	10.29	10.51
P	10.00	10.54	10.18	10.10	4.35	0.00	0.00	0.00	0.00	0.00	0.00	7.73	7.55	10.42	10.41	10.44	10.38	10.54
Q	9.83	9.98	10.09	9.52	4.07	0.00	0.00	0.00	0.00	0.00	0.00	3.47	9.93	9.59	9.47			
R	9.43	10.09	10.07	9.51	3.98	0.00	0.00	0.00	0.00	0.00	0.00	3.47	9.93	9.51	9.38			
S	10.14	10.38	10.09	9.58	4.18	0.00	0.00	0.00	0.00	0.00	0.00	3.55	9.43	10.40				
T	9.98	10.27	9.96	9.48	6.93	0.00	0.00	0.00	0.00	0.00	0.00	2.51	11	9.43	10.49	10.48		
U	9.73	10.29	10.17	9.70	7.48	0.00	0.00	0.00	0.00	0.00	0.00	3.53	9.90	10.51	10.41			

LONG POOP DECK



UPPER DECK



1977 AUG - OCT
1981 AUG - SEP
1985 MAR - APR
1986 AUG - SEP

Fig. 3 Replacement of Deck Plate
(47 years old in 1977)

Figure 4 shows the relation between the corrosion ratio δ and the area ratio A_c for plates K-13-P (Table 2) and inner plate of J-13-P (Table 3). Where A_c is the Ratio of A (an area of a portion of concern around corrosion hole or holes imaginarily taken concentrically of it or them), to the area of the whole plate A_s . That is to say $A_c = A/A_s$. The corrosion ratio δ is the mean corrosion volume ratio calculated in the area of concern A stated above. As shown by both curves in Fig. 4, A_c is going to saturate as δ is approaching to 100%. Let us assume that the whole area corrosion rate Δ is the value of δ at $A_c = 100\%$, and that V is the ratio of corrosion hole or holes area to the whole area of the plate. In Fig. 5, two points (vacant circles) show the calculated relation between Δ and δ using Tables 2 and 3. It is natural that $\Delta = 0$ at $V = 0$. Then we get the quadratic curve which passes three points mentioned above as following.

$$V = 7.76 \times 10^{-5} \Delta^2 + 9.97 \times 10^{-2} \Delta \quad (1)$$

We assume that the relation of equation (1) can be applied to the relation of Δ and V for whole ship. Putting $\Delta = 5.00$ in equation (1), we get $V = 0.693$. The corrosion hole rate of 0.693% is very big value. It is because that if there are corrosion holes in the bottom plating it is very dangerous for the ship (*K-maru* had such experience in her life). It can be understood from this analysis that mean thickness reduction rate of 5% at midship (shown in Table 1) is not a trivial but a serious matter.

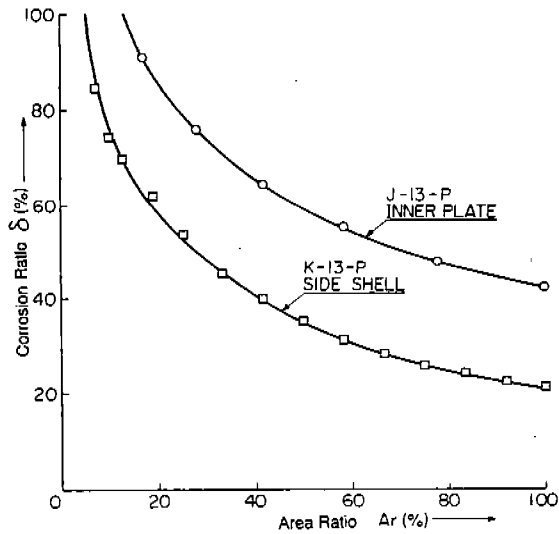


Fig. 4 Relation between Area Ratio A_r and Corrosion Rate δ

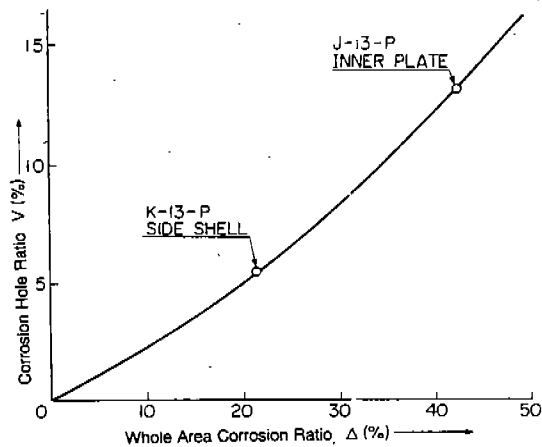


Fig. 5 Relation between Whole Area Corrosion Rate Δ and Corrosion Hole Ratio V

DEFORMATION OF HULL

Measurements of ship hull deformation of *K-maru* were conducted at the time of her docking. Hull deformation was determined by measuring the distances between points on the hull and their projections on the plane containing a line which passed two end points of original straight keel line and four lines which extended horizontally from both side from previous two points. Transits, strings with weights, levels and tape measures were used for measurement.

Deformation measurements of bulkheads were conducted based on a horizontal base line connecting two points, each on a touching line of a bulkhead end to side shell.

Table 4 shows vertical and transverse deformations of the keel at square stations SS0 (stern) through SS9 (close to stern). A little amount of overall deformation to starboard side can be observed. The vertical deformation is dependent on positions of blocks.

Table 4. Deformation of Keel

Measured Position	SS0	SS1	SS2	SS3	SS4	SS5	SS6	SS7	SS8	SS9
Vertical Displacement	0	-24	-31	-34	-41	-26	-31	-28	-10	0
Transverse Displacement	0	95**	135	215	215	225	205	145	3.55	0

** Displacement of Keel at Starboard Side

Figures 6 and 7 show horizontal deformations of side plates at the height from the keel line to be 4m (4WL) and 7m (7WL). In the figures, (+) indicates outward and (-) indicates inward deformations. At 4WL, there are little horizontal deformations around midship (at SS4 and SS5). And there are outward deformations at bow side and a little bit inward deformations at stern side. At 7WL, quite different from deformations at 4WL, whole deformations occur to port side direction. The maximum deformation at 4WL is 302 mm and this value corresponds to 2.3% of the breadth.

Deformation measurements of a bulkhead at Fr.60 (not far from midship = Fr.64 1/2) show that the maximum deformation is 26 mm which is equal to 0.20% of the ship breadth at the position. This value is negligible small from a view point of the reduction in buckling strength.

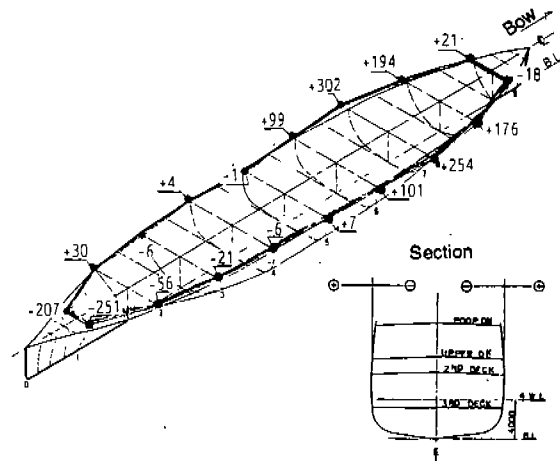


Fig. 6 Deformation of Side Shell at 4WL

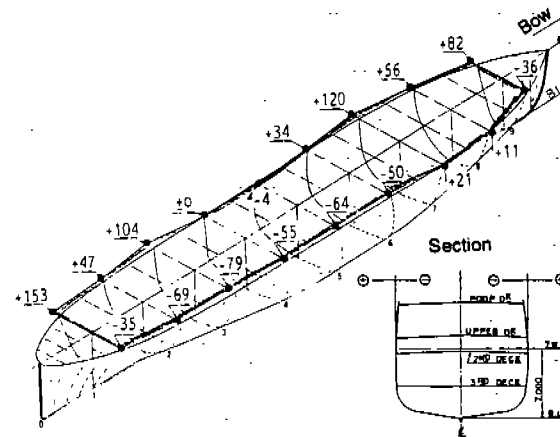


Fig. 7 Deformation of Side Shell at 7WL

Other than mentioned above, deflections of the bulkhead at Fr.116 (not far from stem), vertical deflections of side lines of the upper deck and the overall deflections of the long poop deck were measured. In the measurements of the long poop deck, the maximum upward deflection was 89 mm, the maximum downward - 202 mm. And it was revealed that there were slow humps and hollows all over the decks.

It is considered that deformations measured are piled up due to so many times of long navigations, repairs of the rivet ship by welding, and unbalanced replacements of port and starboard sides shell plates. Especially the unbalanced replacements mentioned above are considered to be the reason of the deformation of the keel line. It is considered to be impossible to repair these deformations.

CHARACTERISTICS OF OLD PLATE

Side shell and deck plates of *K-maru* (here after called "old plates"), which were replaced by new ones at the time of her repair docking, were carefully examined on such items as chemical compositions, static tensile strength, fracture toughness, Charpy impact strength and fatigue strength. Plate thickness and surface roughness measurements were also conducted on plates with excessive corrosion.

Chemical compositions

Table 5 shows chemical compositions of four old shell plates (named SS-1 through SS-4) with those of a commercial steel NK-KA. Old plates show that they have wide variations in an amount of carbon contents. Sulphur contents of them show the critical value or well over the value of the standard for NK-KA. Because of the fact that both carbon and sulphur contents of the plate SS-2 were very high, effects of these high contents on the properties of strength were investigated.

High contents of sulphur was also revealed by a so called sulphur print. Table 6 shows carbon equivalents C_{eq} of SS-2, by which weldability of the steel can be determined. C_{eq} 's of other steel plates with the NK-KA grade commercial steel of today are also calculated and shown in Table 6 and Fig. 8 (diagram to determine conditions of welding based on C_{eq} and plate thickness to be welded). C_{eq} 's are calculated by the following equation, neglecting the contents of chrome, molybdenum and vanadium.

$$C_{eq} = C + Mn / 6 + Si / 24 \quad (2)$$

Figure 8 indicates that the welding of SS-2 should be done by limited conditions.

Table 5. Chemical Compositions

Material	Chemical Compositions (%)					
	C	Si	Mn	P	S	Cr
Standard of NK-KA	0.23 max 0.18 min	0.35 max 0.17 min	2.5C max 1.0C min	0.040 max 0.022 min	0.040 max 0.011 min	—
Commercial	0.12	0.17	0.57	0.022	0.011	—
SS-1	0.18	0.037	0.46	0.018	0.039	—
SS-2	0.33	0.007	0.46	0.044	0.053	0.040
SS-3	0.17	0.029	0.50	0.036	0.049	—
SS-4	0.17	0.048	0.52	0.024	0.045	—

Table 6. Carbon Equivalent

Material	Carbon Equivalent C_{eq} (%)
KA (Commercial)	0.222
SS-1	0.262
SS-2	0.407
SS-3	0.255
SS-4	0.259

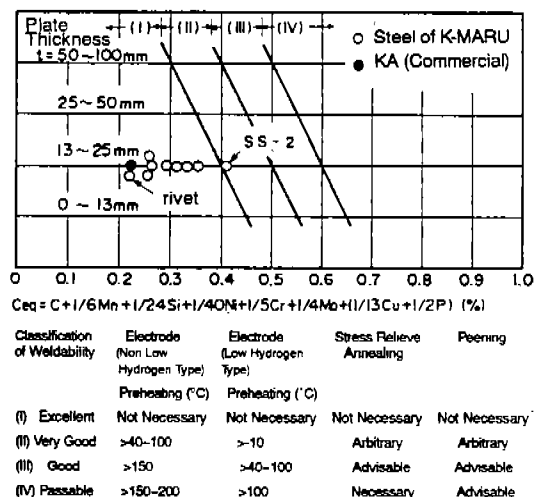


Fig. 8 Welding Conditions of Steel Plate Used Based on Carbon Equivalent [1]

Static tensile strength

Static tensile test were conducted for 17 pieces of test specimens of JIS 13A type (parallel part length = 120 mm, breadth = 20 mm, distance for elongation measurement = 80 mm, over all length = 340 mm). Five old plates (2 side shell plates and 3 deck plates) were used for test specimens. Surfaces of test specimens were as corroded or slightly shaved on an enormously corroded side for the convenience of testing. Test speed settled between chucks of testing machine was 1 mm/min. Test results for steel plates SS-2 and SS-3 are shown in Table 7. It should be noted that test specimens of SS-2 fractured by brittle mode at room temperature of 10°C. No clear yield points were shown at SS-2 specimens. Test specimens other than SS-2 fractured by ductile mode. For these specimens, the yield strength σ_y (calculated at minimum area section between two points for elongation measurement) was 23.1-29.0 kgf/mm² (226 - 284 MPa), and tensile strength σ_b (calculated same manner as σ_y) was 41.3-48.3 kgf/mm² (405 - 473 MPa). And these values were within the specified value of NK-KA ($\sigma_y \approx 24$ kgf/mm² = 235 MPa, $\sigma_b = 41 - 50$ kgf/mm² = 402 - 490 MPa) as shown in Table 7.

Table 7. Mechanical Properties

Material	Yield Strength σ_y (kgf/mm ²)	Tensile Strength σ_b (kgf/mm ²)	Elongation ϵ (%)	Note
SS-2 TP1	—	52.7	12.2	Brittle
SS-2 TP2	—	54.4	13.8	Brittle
SS-3 TP1	27.5	45.4	29.3	Ductile
SS-3 TP2	26.2	44.0	34.1	Ductile
NK Standard	37.0	49.4	33.7*	As Rolled

* Distance Measured 200mm

Photographs 1 and 2 show SEM fractographies of SS-2 (brittle fracture) and SS-3 (ductile fracture) specimens. In Photo 1, a origin of brittle fracture is shown. The ductile fracture pattern shown at lower left hand side of the photo changes to brittle one at the origin. All fracture surface is covered by dimple pattern in case of Photo 2 (SS-3).

Fracture toughness test was conducted for the plate SS-2 which showed brittle mode at static tensile test at room temperature.

Dynamic tensile tests were conducted at strain rate of 0.09-0.13 /sec, at temperatures 0°C and 18±2°C. For SS-2 specimen,

almost all surface was observed as brittle mode at 0°C. At 20°C, almost all surface was observed as ductile mode and only limited parts showed crystalline fracture surface of brittle mode. Results of dynamic tensile tests almost corresponded to those of static tests, excepting that specimens with very rough surface due to corrosion fractured by ductile mode with relatively small value of elongation ϵ of 20% (mean value of ϵ for specimens by ductile mode was 31%, by brittle mode - 12%). It is considered that the effects of stress concentration due to corrosion revealed itself strongly at dynamic tests.

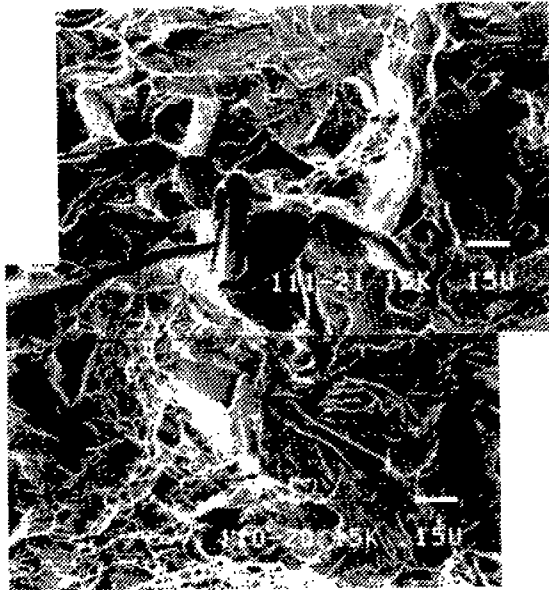


Photo 1. Fractography of SS-2

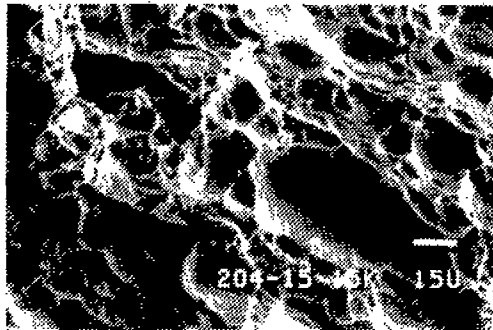


Photo 2. Fractography of SS-3

Charpy and fracture toughness test

Charpy impact tests were conducted for the old plates SS-2, SS-4 and commercial steel plates of NK-A grade with a thickness of 12 mm. Two mm V notch and full size specimens were used. Specimens were so made that their direction was coincident with their rolled direction (shown by letter L in Table 8) or perpendicular to them (shown by letter C). Table 8 shows results of impact tests as T_s (fracture transition temperature) and T_{35} (temperature corresponding to energy consumption of 35 ft-lbd = 4.8 kg-m). Steels SS-2 and SS-4, having been rolled without consideration of their weldability, and so called rimmed steel, show very low value of T_s ,

T_{35} and E_o as compared to those of steels used today. Especially SS-2, fractured by brittle mode in static tensile test, show very low values (out of evaluation) of T_s and T_{35} , 1/10 (C direction) to 1/45 (L direction) value of E_o . This means that there is a possibility of unstable propagation of cracks initiated at weld defects.

Fracture toughness tests were conducted for SS-2. As the original thickness of SS-2 was 0.52 inch (13.21 mm) and was heavily corroded, it was impossible to conduct the perfect fracture toughness test by CT test specimen. And so modified specimens shown in Fig. 9 were used.

Mechanical notch specimens with a tip radius of 0.2 mm were tested at 18°C, 0°C, -20°C, -40°C by testing speed of 20 mm/sec. One specimen, which had a notch size of 2.5mm in depth with a fatigue crack, was tested at -20°C.

Figure 10 shows the results. The solid line in the figure shows the transition curve connecting lower bound of experimental data values of specimens with mechanical notches. The broken line in the figure corresponds to the transition curve for specimens with fatigue crack, being obtained by shifting the solid line to higher temperature side by 30°C [2]. In the case that an experimental value of K_{Ic} is equal to K_{Ic} , the thickness t of the specimen satisfies the following equation.

$$t \geq 22 (K_{Ic} / \sigma_y)^2 \tag{3}$$

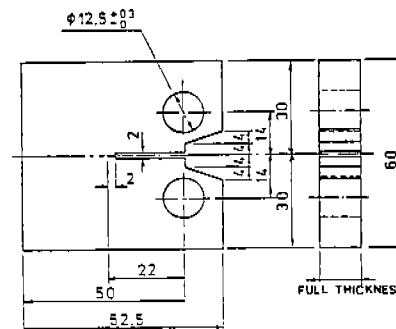


Fig. 9 Test Specimen for CT Test

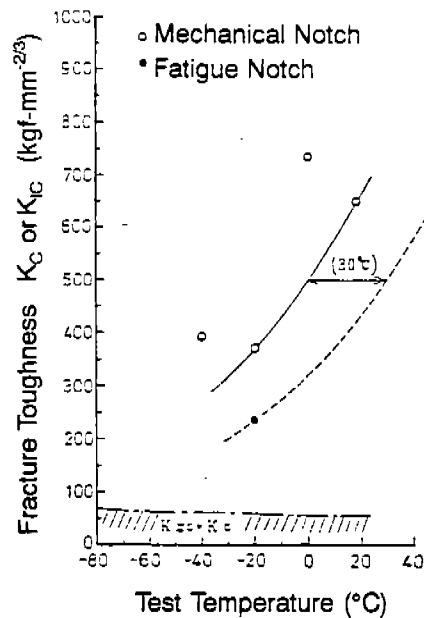


Fig. 10 Temperature Dependency of Fracture Toughness K_{Ic} of SS-2

Table 8. Charpy Impact Test Results

Material	Thickness	Chemical Compositions (%)					Direction	Impact Test Results		
		C	Si	Mn	P	S		T ₁	T ₂	E _{1/2}
NK-A Grade Commercial Steel (Material A)	12 mm	0.13	0.28	0.77	0.016	0.010	L	-16°C	-32°C	27.0 kgf-m
							C	-2	-19	7.2
NK-B Grade Commercial Steel (Material B)	12 mm	0.12	0.30	0.79	0.017	0.013	L	-11	-30	16.2
							C	-3	-5	5.8
SS-2	12 mm	0.33	0.07	0.46	0.044	0.053	L	> +60	> +60	0.6
							C	> +60	> +60	0.6
SS-4	14 mm	0.17	0.18	0.52	0.024	0.045	L	+32	+9	2.6
							C	+42	-42	2.4

Assuming, in the equation (3), that $t = 12$ mm and $\sigma_y = 25.8$ kgf/mm², then we get the following result

$$K_{Ic} \leq 56.5 (\text{kgf}\cdot\text{m}^{-3/2}) \quad (4)$$

The region of $K_{Ic} = K_{Ic}$ for wide range of temperature can be calculated as shown by the shaded area in Fig. 10, assuming temperature dependency of σ_y as equation (5)[3] and conducting the same calculation as equation (4).

$$\sigma_{yT} = \sigma_{yR} \cdot \exp [(329.6 - 66.5 \ln \sigma_{yR}) (1/T_k - 1/293)] \quad (5)$$

Where,

- σ_{yT} = yield strength (kgf/m²) at temperature of T_k K
- σ_{yR} = yield strength (kgf/m²) at temperature of 293 K.

The fracture toughness of SS-2 can be discussed based on the results obtained hitherto. By using the absorbed energy, E_T (kgf-m) of Charpy impact test at temperature T , K_{Ic} can be calculated by using the equation by Rolfe et. al. as following.

$$K_{Ic} = 120 (\sqrt{E_T})^{3/4} \quad (6)$$

K_{Ic} value in Fig. 10 can be transformed into K_{Ic} by using the following equation in consideration of plate thickness effects on K_{Ic} [4].

$$\begin{aligned} K_{Ic} &= K_{Ic} / F(t) \\ F(t) &= 1 + 0.043 (40-t) \\ (t \leq 40 \text{ mm}) \end{aligned} \quad (7)$$

In Fig. 11, K_{Ic} value calculated by the equation (6) (curve I), K_{Ic} value by the equation (7) (curve III), K_{Ic} for commercial steel plate (curve II) and also K_{Ic} value obtained from CT test as shown by the broken line in Fig. 10 (curve IV), are shown.

Though the CT test shows no fracture toughness values (K_{Ic}) which satisfy K_{Ic} conditions, there is a possibility of a crack propagation under not far from K_{Ic} conditions, in case of crack existence in structural members with large structural constraints.

The stress intensity factor K_I in the case of a crack ($2c$ in length) in infinite plate under uniform tensile stress σ as shown in Fig. 12 is expressed as follows.

$$K_I = \sigma \sqrt{\pi c} \quad (8)$$

For SS-2, the crack length, at which K_I in the equation (8) becomes K_{Ic} (brittle fracture may occur at this value) can be obtained by using curve I and III in Fig. 11. Results are shown in Table 9, assuming working stress σ to be 10 and 20 kgf/m². Under condition of 10°C and $\sigma = 10$ kgf/m², $2c$ is 92 mm or 44 mm. These values are less than 100 mm (considered to be the critical crack length to be found by naked eye inspection), and there are possibilities that such cracks exist in plates equivalent to SS-2 not found by inspection. Such a case is very dangerous for *K-maru*.

Table 9. Critical Length of Defect (Corresponding to 2C in Fig.12)

Temperature	2C crit			
	$\sigma = 10$ kgf/mm ²		$\sigma = 20$ kgf/mm ²	
	For I in Fig.11	For III in Fig.11	For I in Fig.11	For III in Fig.11
0°C	20 mm	65 mm	5.1 mm	16 mm
10°C	44 mm	92 mm	11 mm	23 mm

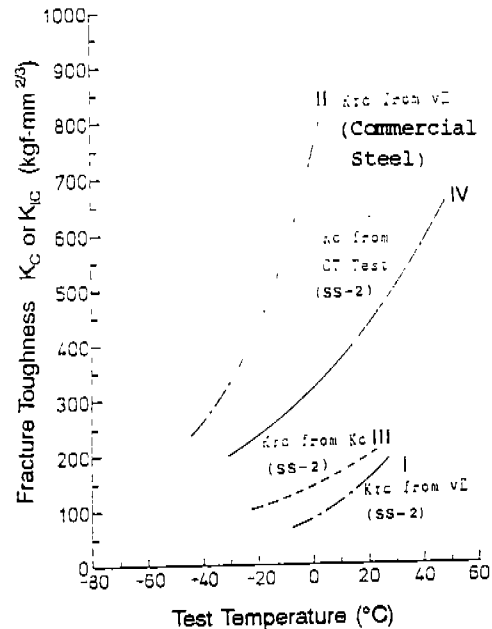


Fig. 11 Comparison of Fracture Toughness of SS-2 and Commercial Steel of NK-A Grade



Fig. 12 Model of Defect in Infinite Plate

Fatigue test

In order to discuss on the potential damages caused by connecting old plate and new ones by welding, also in order to investigate into the effects of corrosion in old plates on the fatigue strength of them, fatigue tests were conducted by using specimens from old plates DP-1 (deck plate). Fig. 13 shows the configuration of specimen used. A new weldable mild steel SM41A plate and a old plate were connected by welding for one type of specimen ("A" type, 10 specimens of this type were tested). For the other type, two new SM41A plates were welded ("B" type, 6 specimens of this type were tested). Single-V groove, 3 passes from one side and 2 passes from the other side were used for welding. The welding conditions were; diameter of electrode = 4 mm, voltage = 20 - 25 V, current = 150 - 180 A and travelling speed = 133 mm/sec. Plate thickness of a new plate and welding conditions were similar to those used at repair works of *K-maru*.

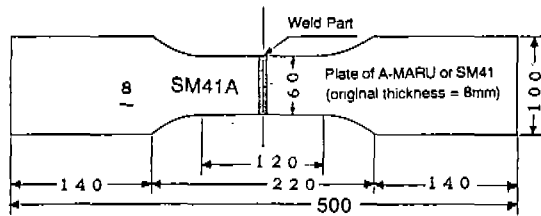


Fig. 13 Fatigue Test Specimen

Figure 14 shows the fatigue life diagram expressed by a load and a nominal stress. Figure 15 shows the fatigue life diagram expressed by a stress at the section with a minimum sectional area. Number C-1, C-2 etc. in Figures 14 and 15 are test specimen numbers. If a welding is sound enough, fatigue cracks in a butt weld joint specimen of SM41A initiate at weld toe and propagate to the thickness direction. But in the "B" type specimens tested, because of relatively large insufficient penetration of weld metal, fatigue cracks initiated at weld defects and propagated in weld metal to final failure. In spite of the fact that the same welding was used for "A" type specimen, fatigue cracks initiated at several points simultaneously on a corroded surface of a old plate and propagated to a thickness direction of a plate to final failure, with one exception (specimen C-4). It could be observed from macro fracture surfaces that many fatigue cracks initiated at many parts in a rough corroded surface and they merged gradually into one and proceeded to a final failure.

Figures 16, 17 and 18 show the enlarged appearances of corroded surface of same test specimens shown in Figures 14 and 15. One side of the plate DP-1 (deck) was, at the time of usage as a

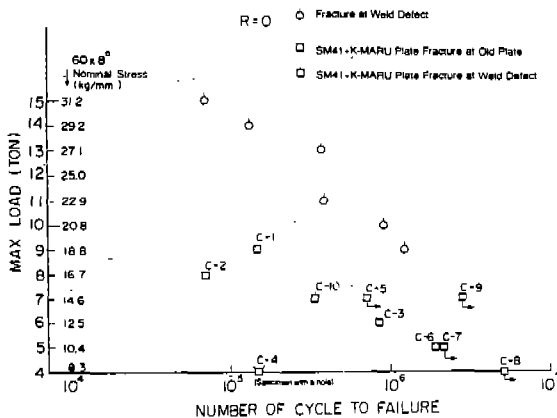


Fig. 14 Fatigue Life Diagram Expressed by Load Applied

part of a hull of *K-maru*, exposed directly to inside of the ship and so protected by many accumulated paint layers. This side of the plate was not corroded and kept a flat surface. But the other side of the plate was under a wooden deck and not protected against corrosion. And so, part of this side were excessively corroded.

In specimen C-3 (Fig. 16), plate thickness decreases gradually to its longitudinal direction. In C-4 (Fig. 17), decrease in thickness is very large and there is even a corrosion hole. In C-6 (Fig. 18), plate thickness shows abrupt changes. In case of C-4, a crack initiated at the edge of the hole played as one of cracks initiated at many points on a corroded surface.

From these results and discussions, we estimate that the reduction in fatigue strength of corroded plates is due to the combined effects of reduction in plate thickness and surface roughness produced by corrosion. From the fact that cracks initiate at corroded surface and propagate in corroded plates even in case of a poor welded joint specimen, the reduction in strength due to plate thickness decrease and rough surface caused by corrosion is more significant from the navigation safety of *K-maru* than the effects of welding of rimmed steel plates on the strength.

DISCUSSION ON NAVIGATION SAFETY

Basic concept on ship hull strength

There are several view points of strength of structures. One view is to assume that individual member consisting a structure works additively to the total strength of the structure (hereafter this view is called "static strength"). Another view is to assume that a crack initiates at the weakest part in a structure and the crack propagates through each structural member independently to other members to final failure (typical case of this is the brittle fracture strength). Other than these, there is a view of strength against emergencies such as collisions or groundings as in cases of ships.

Static strength

Static strength of a ship as a whole can be discussed based on her I/Y value and buckling strength. From the measurement of deterioration due to corrosion at midship of *K-maru*, it is considered that the reduction of I/Y due to deterioration is nearly 5% assuming that there is negligibly small amount of shift of the neutral axis. But there are possibilities of reduction in local buckling strength due to local severe corrosion and deformations.

Brittle fracture

There remains a possibility that there, in *K-maru*, are included such plates with low fracture toughness as the old plate

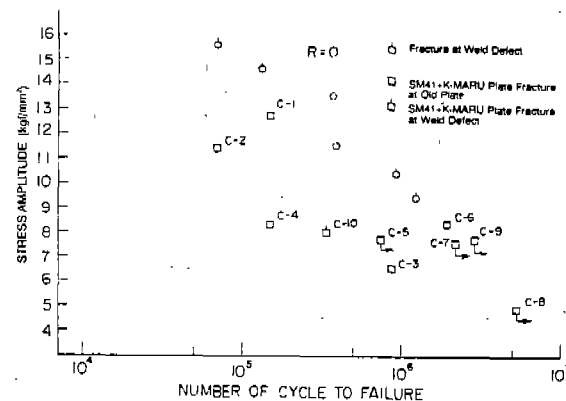


Fig. 15 Fatigue Life Diagram Expressed by Stress at Section with Minimum Section Area

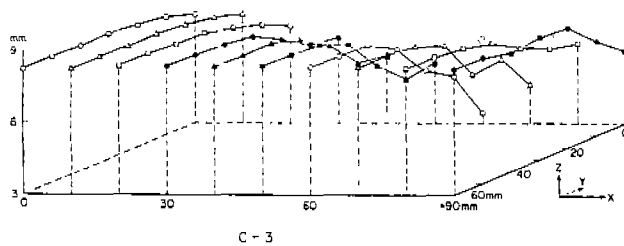


Fig. 16 Appearance of Corroded Surface (Test Specimen C-3)

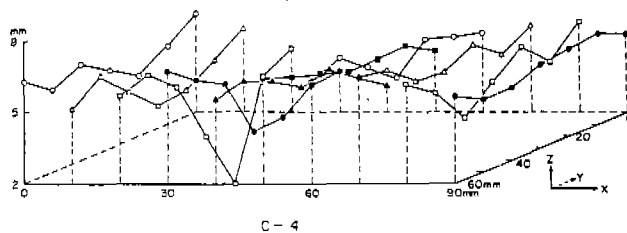


Fig. 17 Appearance of Corroded Surface (Test Specimen C-4)

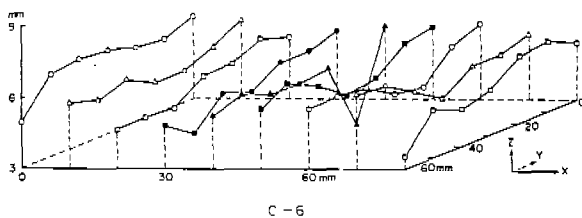


Fig. 18 Appearance of Corroded Surface (Test Specimen C-6)

SS-2, and if repairs of the plates by welding are continued to do, it is possible that brittle fracture might initiate from fatigue cracks from corroded surface or from those due to welding not found at the time of inspections. The latter cracks are invited by use of welding which is not anticipated at the time of the construction of *K-maru*.

Navigation safety

When it comes to discuss the navigation safety or seaworthiness of *K-maru*, not only static and brittle fracture strength, but also strength distribution effects of excessively corroded parts and holes in plates of hull on the strength of the ship, and also the safety at emergencies are to be taken into consideration.

The strength distribution can be expressed by using S/P . Where S is the strength of individual member of a structure and it is a decreasing function of time. P is the external force acting on members and it is independent of time in case that the ship keeps the same navigation conditions over her life. Plate thickness reduction and surface roughness due to corrosion, generations of cracks and deformations of individual member should be considered for the evaluation of S . Tensile, compressive and repeating loads are to be adopted for P . Figure 19 shows the conceptual view of S/P distribution. As time passes, the S/P distribution around M_0 (solid line) at initial stage of a ship shifts to the distribution around M_1 (broken line). In this concern, *K-maru* is considered at the stage of so called wear out failure in the bath tub curve of ship age to failure pattern diagram (Fig. 20 [5, 6]). And even if she were carefully repaired, the S/P distribution described in Fig. 19 continues to shift apart from M_0 and the peak value of the distribution also continues to decrease.

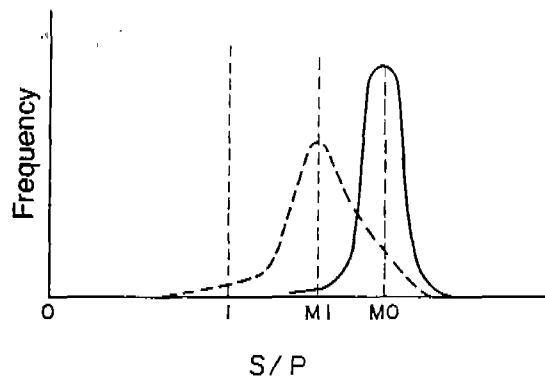


Fig. 19 Conceptual Illustration of Strength Distribution

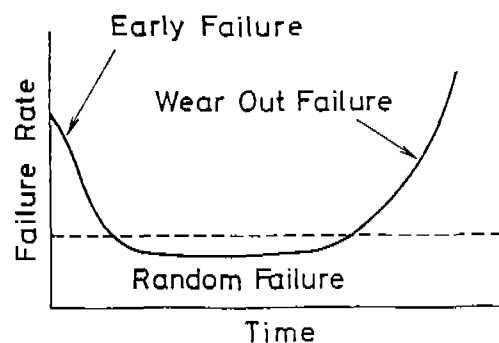


Fig. 20 Relation Between Ship Age and Its Failure Pattern (So called bath tub curve)

Corrosion holes in shell plates under water line directly induce the flooding of water to the ship, and these in deck plates are visible for crew and passengers. Therefore the existence of corrosion holes give heavier influence to the crew members of *K-maru* than the true influence on the strength reduction due to these holes. So the 0.693% of vacant hole ratio estimated from 5% of whole area corrosion ratio has a serious meaning for seaworthiness of *K-maru*.

Navigation safety at emergency should also be considered other than safety at usual time as mentioned above. Here is an example of a marine accident of a very old ship as *Admiral Nakhimov* (17053-ton, 61-year-old). This accident happened at midnight at the Black Sea on August 31 1986. *Admiral Nakhimov*, Soviet passenger ship, collided with a cargo ship *Pyotr Vasev* (41000-ton) and barely 8 minutes later sunk in water [6, 7]. It can be estimated, from the phenomenon shown by *Admiral Nakhimov*, that, at the time of emergency, fractures of *K-maru* can proceed very quickly because of simultaneous effects of reduction in plate thickness, rough surface, cracks, overall and local deformation. It seems to be impossible to keep the safety of *K-maru* at her emergency.

CONCLUSION

Article 1 of Ship Safety Law (Japan) says "ships of Japan should not be used for navigation if their seaworthiness is not guaranteed and not equipped with facilities necessary for keeping safety of lives stipulated by this law". It is considered that the seaworthiness of the ship is guaranteed by such facilities stipulated by Article 2 of

this law as hull, machinery, life saving, living and electric ones. *K-maru* which is equipped with those facilities as mentioned above, and there seems to be nothing to be considered for safety as far as the law is concerned. But it is questionable, however, that the law can be applicable directly to such a long life ship as *K-maru*. Steel plates, used at the time of construction of *K-maru*, were rimmed ones and they were connected by rivets. But today, they are changed to killed steel plates and connections by welding. These changes give great influences to the seaworthiness of *K-maru* which has been used for so long time by repairing so many times and places. Therefore we discussed the safety of *K-maru* not based on Ship Safety Law but on the theories and experiences established today, and concluded that the safety of *K-maru* in future could not be guaranteed.

Other than articles concerning seaworthiness of the ship, Ship Safety Law has Article 13, which says "if more than 10 crew members in a ship appeal the serious defects with reference to seaworthiness, living and other life saving facilities referring to stipulations in this law, the government office concerned should make the necessary investigations and, if necessary, give punishments stipulated by Paragraph 3, Article 12 (suspension of navigation and other punishments)". From this view point, vacant holes due to corrosion, which may give big psychological effects to crew on the safety of their ship, should be considered more seriously than it is estimated theoretically.

Authors are very grateful for government officers con-

cerned who have given us such precious opportunities as to make through investigations of a very long life ship of *K-maru*.

REFERENCE

- 1) H. Suzuki, "Welding Handbook, Junior", revised edition, San-kaido Publishing Co. Ltd. P.506, 1977.
- 2) Japan Welding Association, Final Report of TM Committee Cooperative Research, 1975.
- 3) Japan Welding Society Steel Technology Committee BE Subcommittee, Report of Bond Embrittlement in Weldable Steel Plate, 1975.
- 4) I. Ito, K. Tanaka and M. Sato, "Effect of Plate Thickness on Brittle Fracture Initiation from Surface Notch in Weld Fusion Line and Correlation between the Results of Large Scale Test and Those of Charpy Test" Journal of the Society of Naval Architects of Japan, vol. 131, P. 340, 1972.
- 5) Y. Akita, "Reliability Analysis in Strength of Ships (1st Report)", Journal of SNAJ, vol. 155, PP.207-214, 1984.
- 6) For example, S. Abe, "Hull Damages and Maintenance Measures of NK Registered Ships", Transactions of Nippon Kaiji Kyokai, No. 175, PP. 18-32, 1981.
- 7) For example, First Page of News Paper YOMIURI, Sept. 3, 1986.
- 8) J. O. Jackson, "Death in the Black Sea", TIME, PP. 16-17, Sept. 15 1986.